Published in final edited form as:
Environ Sci Technol. 2012 September 4; 46(17): 9406–9411. doi:10.1021/es301136d.

Formation and Stabilization of Combustion-Generated, Environmentally Persistent Radicals on Ni(II)O Supported on a Silica Surface

Eric Vejerano, **Slawomir M. Lomnicki**, and **Barry Dellinger**
Louisiana State University, Chemistry Department, 232 Choppin Hall, Baton Rouge, LA 70803, United States

Abstract

Previous studies have indicated Environmentally Persistent Free Radicals (EPFRs) are formed when hydroxyl- and chlorine-substituted aromatics chemisorbed on Cu(II)O and $Fe(III)_2O_3$ surfaces and were stabilized through their interactions with the surface metal cation. The current study reports our laboratory investigation on the formation and stabilization of EPFRs on an Ni(II)O surface. The EPFRs were produced by the chemisorption of adsorbates on the supported metal oxide surface and transfer of an electron from the adsorbate to the metal center, resulting in reduction of the metal cation. Depending on the temperature and the nature of the adsorbate, more than one type of organic radical was formed. A phenoxyl-type radical, with g-value between 2.0029 and 2.0044, and a semiquinone-type radical, with g-value from 2.0050 to as high as 2.0081, were observed. The half-lives on Ni(II)O were long and ranged from 1.5 to 5.2 days, which were similar to what were observed on $Fe(III)_2O_3$,. The yields of the EPFRs formed on Ni(II)O was ~ 8x higher than on Cu(II)O and ~50x higher than on $Fe(III)_2O_3$.

Introduction

The relationship between the exposure to airborne fine particles (PM2.5) and chronic disease has been the subject of many studies, but, due to the complexity of the composition of fine particles, the direct mechanism of PM2.5 toxicity has proven elusive [1, 2]. Transition metals are thought to mediate production of reactive oxygen species (ROS) and have been implicated in the toxicity of particulate matter (PM) [3–5].

Copper and iron are usually the highest concentration metals in airborne PM2.5 [6–8], with typical concentrations of 31.7 and 44.6 μg/L, respectively [9]; however, nickel is usually a significant component. Nickel is recognized as a potential human carcinogen [10, 11], can cause allergic reactions [12, 13], and can induce cancer in animals [13, 14]. Nickel in airborne PM is mainly derived from rock weathering and volcanic eruptions, but may also originate from combustion of oil additives and metallurgical processes [15, 16]. In fly ash, nickel has been reported at 240 mg/kg and its concentration in ambient urban air particulate matter ranges from 5 to 50 ng/m^3 [17]. A clear link between the concentration of nickel in airborne particulate matter and combustion of heating oil has been identified [18]. Nickel is also a significant component of the oil used in the steam generating units of power plants (30–40 mg/Kg), which results in Nickel stack emissions of up to 1000 ug/Nm^3 [19, 20]. Importantly, Nickel in ambient PM has been observed to correlate with symptoms of

Supporting Information Available
Figure S1: Examples of spectral deconvolution of EPR signals from Ni(II)O/silica dosed with CT, HQ, PH, 1–2-DCBz, MCBz, and 2-MCP.

respiratory distress, such as wheeze and cough [21]. Chemical analyses suggest nickel exists as metal, sulfides, and oxides, with the oxide accounting for ~50% of the total nickel in airborne PM [17].

Previous studies with Cu(II)O and $Fe(III)_2O_3$ supported on silica particles demonstrated that chlorine- and hydroxyl-substituted aromatics chemisorb to the metal oxide surfaces in combustion and thermal processes under post-flame conditions between 150 and 400 °C. Electron transfer from the adsorbate to the metal ion center results in concomitant formation of an environmentally persistent free radical (EPFR) and reduction of the metal cation [22]. Biochemical and biomedical studies of copper-EPFR complexes indicated these surface-associated EPFR-metal complexes are potent ROS generators, resulting in pulmonary and cardiovascular dysfunction in mouse and rat models [23] [24]. Our reports of EPFR-metal complexes suggest a new mechanism of cardiopulmonary dysfunction due to induction of oxidative stress induced by catalytic cycles involving the EPFRs and reduced metals [25]. Nickel, like iron and copper, may act as a surface catalyst where EPFRs can be formed and stabilized upon adsorption of organic compounds.

In this manuscript, we report the results of a laboratory study of the formation, structure, and persistence of EPFRs formed from aromatic molecular adsorbates on particles consisting of 5% Ni(II)O on silica. Since they are common by-products of combustion processes and have been previously proven to form EPFRs, catechol, 1,2-dichlorobenzene, monochlorobenzene, 2-monochlorophenol, hydroquinone, and phenol were selected as potential precursors/adsorbates.

Experimental

Surrogate sample synthesis

Samples (5% Ni(II)O (3.9% Ni) by weight supported on silica) were prepared by impregnation of silica gel with nickel (II) nitrate hexahydrate (Sigma-Aldrich, nickel (II) nitrate hexahydrate, 99+%) using the method of incipient wetness followed by calcination. Silica gel powder (Sigma-Aldrich, grade 923, 100–200 mesh size) was introduced in a sufficient amount into a 0.378 M aqueous solution of the nickel (II) nitrate for incipient wetness to occur. The resulting suspension was allowed to equilibrate for 24 h at room temperature and dried at 120 °C for 12 h before calcination in air for 5 h at 450 °C.

EPFR formation experiments

The adsorbate chemicals, catechol—CT (Aldrich, 99+%), hydroquinone—HQ (Aldrich, 99+%), phenol—PH (Aldrich, 99+%), 2-monochlorophenol—2-MCP (Aldrich, 99+%), monochlorobenzene—MCBz (Aldrich, 99.8% anhydrous), and 1,2-dichlorobenzene—1,2-DCBz (Sigma-Aldrich, 99% HPLC grade) were used as received without further purification.

The particulate samples were exposed to the vapors of the adsorbates using a custom-made vacuum exposure system [22], consisting of a vacuum gauge, dosing vial port, equilibration chamber, and 2 reactors. Prior to adsorption, the supported metal oxide sample was activated in air *in situ* at 450 °C for 30 min. Vapors of the molecular adsorbates were introduced into the equilibration chamber at the desired pressure (~10 Torr), and the particles were exposed to the adsorbate vapors for 5 min over the selected temperature (150 to 400 °C). Upon completion, the port and dosing tube were evacuated for 1 h at the dosing temperature and pressure of 10^{-2} Torr. The reactor was then sealed under vacuum, and the sample was cooled to room temperature prior to EPR measurements.

Electron Paramagnetic Resonance

All EPR measurements were performed using a Bruker EMX-2.0/2.7 EPR spectrometer with dual cavities, X-band, 100 kHz and microwave frequency, 9.53 GHz. The spectra were obtained at room temperature. The typical operating parameters were: microwave power 1 mW, modulation amplitude 4 G, sweep width 200 G, time constant 40.960 ms, and sweep time 167.7 s. The non-derivative absorption spectra were deconvoluted using the Origin 7E Peak Fitting module. The overall fit was compared with both the original absorption spectra as well as the first-derivative spectra.

Radical decay

Kinetic studies were performed to determine the persistence of the EPFRs in air. EPFR-Ni(II)O/silica samples prepared at 230 °C were continuously exposed to ambient air at room temperature, and the EPR spectrum was measured periodically to determine the radical concentration as a function of time. Some samples were extracted with 1 mL of methanol or dichloromethane for 1 h and subjected to GC-MS analyses to identify molecular products [26]. The particles were dried under vacuum after extraction and the EPR spectra of both the dried particles and the solution extracts were acquired.

Results and Discussion

The adsorption of various aromatic molecular adsorbates on the surface of 5% Ni(II)O/silica particles from 150 to 400 °C resulted in asymmetrical EPR spectra, indicating the presence of one or more types of EPFRs (cf. Figure 1). The EPFR yields from various adsorbates exhibited a maximum at 250–300 °C, with the exception of phenol and monochlorobenzene, which had maxima at 350 °C. Deconvolution of the EPR spectra allowed identification of three different spectral components, denoted as g1, g2, and g3, with g-values of approximately 2.0010, 2.0030, and >2.0045, respectively, as was the case of previously reported EPFRs on copper and iron oxides [22, 27]. The shape of the EPR spectra and the relative intensities of the g1, g2, and g3 signals generally varied with adsorption temperature. Table 1 presents deconvolution results of the spectra obtained for EPFRS formed between 150 and 400 °C.

Our previous studies with copper and iron have shown EPFRs are formed when the molecular adsorbate physisorbs on the metal's surface-hydroxide terminal groups of and chemisorbs by elimination of HCl or H_2O, leading to formation of an organic-metal oxide complex [22, 27]. Concomittant or subsequent electron transfer from the oxygen atom to the metal ion reduces the metal ion and forms a surface-stabilized EPFR. The general scheme for the reaction is presented for 2-monochlorophenol at Ni^{2+} sites on Ni(II)O/silica particle surfaces (cf. Scheme 1)

Metal *F*-center Formation

Previous studies with Cu(II)O and $Fe(III)_2O_3$ on silica particles indicated the formation of an *F*-center, which is an electron trapped in anionic vacancies of the crystal lattice [22, 27]. The deconvolution of their EPR spectra reveals a g1 signal, which we ascribe to the formation of an *F*-center [28]. The *F*-centers are more readily observed from the adsorption of catechol, hydroquinone, monochlorobenzene, and 2-monochlorophenol. The typical g-values of F-centers for the different adsorbates ranged from 1.9970 to 2.0020. 1,2-Dichlorobenzene and phenol showed no detectable amount of *F*-center at all temperatures. The fact that *F*-centers were not detectable for some of the adsorbates does not suggest they are not formed, but rather the limitations of deconvolution to discern the low concentrations of *F*-centers.

g2 and g3 Radical Formation

Depending on the nature of the adsorbates and the number of substituents, one or two type of EPFRS are formed [22]: g2-type signals, which are attributed to a phenoxyl-type EPFRs and g3-type signals, attributed to semiquinone-type EPFRs.

Phenol—Previous studies with phenol on Cu(II)O and $Fe(III)_2O_3$ on silica showed one predominant EPFR was formed. Analyses of the EPR spectra for phenol adsorbed on Ni(II)O/silica exhibited similar behavior. A small asymmetry of the resulting EPR spectra was observed due to the presence of g3 species for adsorption temperature below 300 °C. The observed g2-value oscillated between 2.0035 to 2.0040 for adsorption temperature of 150–400 °C , suggesting a phenoxyl EPFR. Since phenol has only one hydroxyl substituent capable of chemisorbing to form the surface-associated phenoxyl EPFR, this is as expected [22, 27, 29]. However, it is quite surprising to observe the formation of small amounts of g3 species from phenol at adsorption temperatures below 300 °C. The g-value of g3 (<2.0050) suggests the formation of *para*-semiquinone species (cf. discussion of hydroquinone). Such species can be formed by adsorption of the phenol molecule through a parallel orientation to the surface, followed by the reaction of ring carbon with surface hydroxyl. However, parallel phenol adsorption is rather unusual for polar surfaces such as metal oxides and is more typical for metallic surfaces [30]. Calculations of chlorinated phenols adsorption on copper oxides have shown flat adsorption of phenol is possible [31]. As a result, a very weakly-bonded molecular adsorbate complex is formed. However, neither dissociation, nor electron transfer was suggested as the driving mechanism [31]. The absence of *p*-semiquinone radicals above 300 °C indicates an easy decomposition of the flat-adsorbed species.

The phenol EPFR yield increased from 150 to 350 °C and declined at 400 °C. The decrease in EPFR yield above 350 °C was likely due to decomposition of the phenoxyl radical to cyclopentadienyl radical, which is consistent with the reported behavior of phenol on all the metal oxide surfaces [32]. The yield of EPFR from adsorption of phenol is the lowest among all the adsorbates (cf. Figure 2).

Monochlorobenzene—Monochlorobenzene chemisorbs by elimination of HCl, rather than H_2O. Its EPFR yield curve is similar to phenol, but much larger at each reaction temperature above 150 °C. 2-monochlorophenol also formed phenoxyl radicals with g-values ranging from 2.0031 to 2.0038. An analysis of the GC-MS extracts of EPFRs from monochlorobenzene indicated the major molecular product formed at all temperatures was phenol. No EPFRs with g-values in the range of 2.0040–2.0050 were detected; suggesting *p*-semiquinone EPFR was not formed. However, a g3 signal, with higher g-values of ~ 2.0060, was observed at all temperatures but with much higher intensities at temperatures of 300 – 400 °C. (At 230 °C, the g3 g-value was assigned as 2.0081.) The g-values were similar to the those observed on Cu(II)O, but were higher than those reported for $Fe(III)_2O_3$, whose g-value ranged from 2.0053 to 2.0060 [27]. The formation of the *o*-semiquinone-type EPFR occurs much more readily than the *p*-semiquinone EPFR in the case of phenol. Monochlorobenzene upon dissociative chemisorption, releases chlorine which forms surface hypochlorite species [28]. These species are very strong chlorinating agents and result in chlorination of monochlorobenzene to 1,2-dichlorobenzene [28, 33, 34]. A similar reaction was observed for monochlorobenzene on Cu(II)O and $Fe(III)_2O_3$/silica surface [22, 27]. This suggest *in situ* formed 1,2-dichlorobenzene can be a precursor to formation of *ortho*-semiquinone radicals, which is consistent with observed higher g3 values. This is also confirmed by the analyses of the GC-MS extracts of the 300 to 400 °C samples, revealing the presence of 1,2-dichlorobenzene on the sample. Thus, the high g-value signal is attributed to the formation of an *o*-semiquinone-type EPFR. The observed 2.0081 g-value

for one temperature cannot be explained at the moment. Because of a significant shift of g-value, one cannot exclude the contribution of other unidentified radical species formed on the surface.

1,2-Dichlorobenzene and 2-monochlorophenol—1,2-Dichlorobenzene adsorption on a Ni(II)O/silica surface resulted in the highest EPFR yield of all adsorbates below 350 °C (cf. Figure 2) with a maximum yield at 300 °C. EPR spectral deconvolution revealed presence of two adsorbed species: a g2 signal with g-values ranging from 2.0034 to 2.0041, and a g3 signal, with g-values between 2.0050 to 2.0071. In contrast to 1,2-dichlorobenzene, 2-monochlorophenol exhibited monotonic increase in EPFR yields from 150 to 400 °C (cf. Figure 2). 2-Monochlorophenol produced three EPR signals: an *F*-center (g1, as described previously), a g2-type signal with very narrow g-value range of 2.0042 to 2.0043, and a g3-type signal with g-values ranging from 2.0049–2.0059. For both 1,2-dichlorobenzene and 2-monochlorophenol, the g2-type radical was assigned to a 2-chlorophenoxyl radical and the g3 signal to an *o*-semiquinone radical. Based on our previous research, typical g-values for surface bound *o*-semiquinone radicals are 2.005 and higher [22, 27]. For 1,2-dichlorobenzene, the ratio of phenoxyl-type radical to *o*-semiquinone-type radical was constant at ~2 (cf. Figure 3), indicating more phenoxyl species formed. For 2-monochlorophenol, phenoxyl radical yield increased as temperature increased, with a maximum yield at 400 °C, while *o*-semiquinone radical yield remained constant. Species g2 formed from adsorption of 1,2-dichlorobenzene have, on average, much lower g-values (2.0035) compared to those formed from 2-monochlorophenol (2.0045) (cf. Table 1). In the case of g2 radicals formed from 2-monochlorophenol, the presence of the chlorine substituent in the benzene ring is known to increase the g-value, and thus, 2-chlorophenoxyl species formation is consistent with both g-values and the parent adsorbate molecule [28]. In contrast, g2 species formed from 1,2-dichlorobenzene adsorption exhibit a typical g-value for a phenoxyl species. Adsorption of 1,2-dichlorobenzene proceeds through a bidentate species (V) in Scheme 1, forming an *o*-semiquinone radical with significant yield, and its decomposition leads to formation of g2 phenoxyl species. This is consistent with the shift of the maximum yield from 250 °C for g3 to 300 °C for g2.

Catechol and Hydroquinone—The yield of EPFRs from adsorption of catechol on Ni(II)O/silica increased from 150 to 300 °C, followed by a slow decline at higher temperatures. The EPFR yield from hydroquinone adsorption was lower; however, it exhibited a monotonic yield increase with temperature up to 400 °C (cf. Figure 1). EPR spectral deconvolution of catechol adsorption revealed two EPFR signals. The g3 signal for catechol, with g-values from 150 to 400 °C, ranged from 2.0051 to 2.0065, which was consistent with our previous study of catechol adsorption on Cu(II)O and $Fe(III)_2O_3$ [22, 27], and indicated formation of *o*-semiquinone EPFRs. Another EPR signal, g2, with g-values ranging from 2.0031 to 2.0043 was observed at all temperatures. As was the case for adsorption of catechol on Cu(II)O and $Fe(III)_2O_3$, the g2 and g3 EPFR yields were almost equal. A g2-type EPFR was formed, similar to 1,2-dichlorobenzene through decomposition of a bidentate species. This is supported by GC-MS analyses of the EPFR-particle extract, which revealed phenol was a molecular product at all temperatures.

EPR spectral deconvolution revealed only one signal for hydroquinone adsorption, with g-values ranging from 2.0044 to 2.0057, which assigned to a g3-type, *p*-semiquinone radical. The formation of only one signal for hydroquinone was expected and was similar to the study on copper and iron surfaces. The g-value of the g3 signal was similar to the 2.0045–2.0060 reported in the literature for *p*-semiquinone radical anion in solution [35, 36]. The single EPR species from hydroquinone adsorption is consistent with its structure. Assuming perpendicular physisorption, chemisorption will only occur at one of the hydroxyl substituents . Analyses of the GC-MS extracts of hydroquinone showed no formation of

phenoxyl-based molecular products, which further corroborates the EPR spectral assignment.

Persistence and Lifetime of EPFRs

Organic radicals are typically very reactive or unstable and short-lived species. However, we have previously reported radicals bound to copper and iron oxides and formed from selected organic molecules are persistent and are relatively long-lived in the environment, i.e. environmentally persistent.

When exposed to ambient air at room temperature, surface-bound EPFRs associated with Ni(II)O exhibited slow decay (cf. Figure 4). The half-lives of the unchlorinated EPFRs of catechol were ~ 2.8 days. Phenol exhibited two decay regimes - a “fast” decay, with a half-life of 0.56 days, and a second, slow decay, with a half-life of 5.2 days. This was the longest half-life observed for all the adsorbates. Radicals formed from phenol were also observed to have the longest half-lives on copper and iron oxides, suggesting phenoxyl radicals were the least reactive of all the EPFRs. The faster decay is attributed to decomposition of phenoxyl radical to cyclopentadienyl radical on highly reactive surface sites [32].

The half-lives of the EPFRs for the chlorinated adsorbates on Ni(II)O/silica were much longer than the corresponding species on Cu(II)O/silica. The half-lives were: 1.7 days for 1,2-dichlorobenzene, 2.4 days for monochlorobenzene, and 3.8 days for 2-monochlorophenol. The persistency of the radicals on the Ni(II)O surface was 2 orders of magnitude greater than on copper oxide. One has to remember, however, that the observed half-lives are for all the radicals present on the surface. In most cases, a mixture of phenoxyl- and semiquinone-type radicals was present, and it was very difficult to assess the persistency of the individual EPFR species. However, the results suggest the more surface phenoxyl species are formed, the more persistent the EPR signal. This suggests the persistency may be driven by the presence of phenoxyl or chlorophenoxyl radicals.

Supplementary Material

Refer to Web version on PubMed Central for supplementary material.

Acknowledgments

This research was supported by the National Institute of Environmental Health Sciences, Superfund Research Program under Center Grant P42ES013648

Literature Cited

1. Dockery DW, et al. An association between air pollution and mortality in six US cities. N Engl J Med. 1993; 329:1753–1759. [PubMed: 8179653]
2. Pope CA III, et al. Lung Cancer, Cardiopulmonary Mortality, and Long-term Exposure to Fine Particulate Air Pollution. JAMA. 2002; 287(9):1132–1141. [PubMed: 11879110]
3. Gurgueira SA, et al. Rapid increases in the steady-state concentration of reactive oxygen species in the lungs and heart after particulate air pollution inhalation. Environ Health Perspect. 2002; 110(8): 749–755. [PubMed: 12153754]
4. Peters DC, Epstein FH, McVeigh ER. Myocardial wall tagging with undersampled projection reconstruction. Magn Reson Med. 2001; 45(4):562–567. [PubMed: 11283982]
5. Valavanidis A, et al. Electron paramagnetic resonance study of the generation of reactive oxygen species catalysed by transition metals and quinoid redox cycling by inhalable ambient particulate matter. Redox Rep. 2005; 10(1):37–51. [PubMed: 15829110]
6. Mamane Y. Estimate of municipal refuse incinerator contribution to Philadelphia aerosol --I. Source analysis. Atmospheric Environment. 1988; 22(11):2411–2418.

7. Smith KR, Aust AE. Mobilization of iron from urban particulates leads to generation of reactive oxygen species in vitro and induction of ferritin synthesis in human lung epithelial cells. Chemical Research in Toxicology. 1997; 10(7):828–834. [PubMed: 9250418]
8. Demuynck M, et al. Chemical analysis of airborne particulate matter during a period of unusually high pollution. Atmospheric Environment. 1976; 10(1):21–26.
9. Sørensen M, Schins RPF, Hertel O, et al. Transition Metals in Personal Samples of PM2.5 and Oxidative Stress in Human Volunteers. Cancer Epidemiol Biomarkers Prev. 2005; 14:1340–1343. [PubMed: 15894700]
10. Fletcher GG, et al. Toxicity, uptake, and mutagenicity of particulate and soluble nickel compounds. Environ Health Perspect. 1994; 102(Suppl 3):69–79. [PubMed: 7843140]
11. Sunderman, FW. Nickel in the Human Environment. Oxford University Press; 1985. p. 530
12. Costa M, et al. Phagocytosis, cellular distribution, and carcinogenic activity of particulate nickel compounds in tissue culture. Cancer Res. 1981; 41(7):2868–2876. [PubMed: 7248947]
13. Sunderman FW. A pilgrimage into the archives of nickel toxicology. Ann Clin Lab Sci. 1989; 19(1):1–16. [PubMed: 2644888]
14. Costa M, Mollenhauer HH. Carcinogenic activity of particulate nickel compounds is proportional to their cellular uptake. Science. 1980; 209(4455):515–517. [PubMed: 7394519]
15. Greim H, et al. Toxicity of fibers and particles - Report of the Workshop Held in Munich, Germany, 26–27 October 2000. Inhal Toxicol. 2001; 13(9):737–754. [PubMed: 11498804]
16. Golant MB, et al. Klystron Oscillator for 3-Centimeter Range, Stabilized by a Superconducting Resonator. Instrum Exp Tech (USSR). 1969; 3:802.
17. Fuechtjohann L, et al. Speciation of nickel in airborne particulate matter by means of sequential extraction in a micro flow system and determination by graphite furnace atomic absorption spectrometry and inductively coupled plasma mass spectrometry. J Environ Monitor. 2001; 3(6): 681–687.
18. New York City Community Air Survey. New York City: 2010. Nickel concentrations in Ambient Fine Particles: Winter monitoring, 2008–2009. Supplemental report.
19. Galbreath KC, et al. Nickel and sulfur speciation of residual oil fly ashes from two electric utility steam-generating units. Journal of the Air & Waste Management Association. 2005; 55(3):309–318. [PubMed: 15828673]
20. Wang YF, et al. Characteristics of Heavy Metals Emitted from a Heavy Oil-Fueled Power Plant in Northern Taiwan. Aerosol and Air Quality Research. 2010; 10(2):111–118.
21. Patel MM, et al. Ambient Metals, Elemental Carbon, and Wheeze and Cough in New York City Children through 24 Months of Age. American Journal of Respiratory and Critical Care Medicine. 2009; 180(11):1107–1113. [PubMed: 19745205]
22. Lomnicki S, et al. Copper oxide-based model of persistent free radical formation on combustion-derived particulate matter. Environ Sci Technol. 2008; 42(13):4982–4988. [PubMed: 18678037]
23. Balakrishna S, et al. Environmentally persistent free radicals amplify ultrafine particle mediated cellular oxidative stress and cytotoxicity. Part Fibre Toxicol. 2009; 6 p. No pp. given.
24. Lord K, et al. Environmentally persistent free radicals decrease cardiac function before and after ischemia/reperfusion injury in vivo. Journal of Receptors and Signal Transduction. 2011; 31(2): 157–167. [PubMed: 21385100]
25. Khachatryan L, et al. Environmentally Persistent Free Radicals (EPFRs). 1. Generation of Reactive Oxygen Species in Aqueous Solutions. Environ Sci Technol. 2011; 45(19):8559–8566. [PubMed: 21823585]
26. Truong H, Lomnicki S, Dellinger B. Potential for Misidentification of Environmentally Persistent Free Radicals as Molecular Pollutants in Particulate Matter. Environ Sci Technol. 2010; 44(6): 1933–1939. [PubMed: 20155937]
27. Vejerano E, Lomnicki S, Dellinger B. Formation and Stabilization of Combustion-Generated Environmentally Persistent Free Radicals on an $Fe(III)_2O_3$/Silica Surface. Environ Sci Technol. 2011; 45(2):589–594. [PubMed: 21138295]
28. Lomnicki S, Dellinger B. A detailed mechanism of the surface-mediated formation of PCDD/F from the oxidation of 2-chlorophenol on a CuO/silica surface. J Phys Chem A. 2003; 107(22): 4387–4395.

29. Boyd SA, Mortland MM. Dioxin Radical Formation and Polymerization on Cu(Ii)-Smectite. Nature. 1985; 316(6028):532–535.

30. Lezna RO, et al. Adsorption of phenol on gold as studied by capacitance and reflectance measurements. Langmuir. 1991; 7(6):1241–1246.

31. Altarawneh M, et al. A first-principles density functional study of chlorophenol adsorption on Cu(2)O(110):CuO. J Chem Phys. 2009; 130(18)

32. Khachatryan L, et al. Formation of Cyclopentadienyl Radical from the Gas-Phase Pyrolysis of Hydroquinone, Catechol, and Phenol. Environ Sci Technol. 2006; 40(16):5071–5076. [PubMed: 16955909]

33. Bandara J, Mielczarski JA, Kiwi J. I. Adsorption mechanism of chlorophenols on iron oxides, titanium oxide and aluminum oxide as detected by infrared spectroscopy. Appl Catal B-Environ. 2001; 34(4):307–320.

34. Farquar GR, et al. X-ray spectroscopic studies of the high temperature reduction of Cu(II)O by 2-chlorophenol on a simulated fly ash surface. Environ Sci Technol. 2003; 37(5):931–935. [PubMed: 12666923]

35. Hales BJ, Case EE. Immobilized radicals. IV. Biological semiquinone anions and neutral semiquinones. Biochim et Biophys Acta, Bioenerg. 1981; 637(2):291–302.

36. Yonezawa T, et al. Solvent effects on the g factors of semiquinones. Bull Chem Soc Jap. 1970; 43(4):1022–1027.

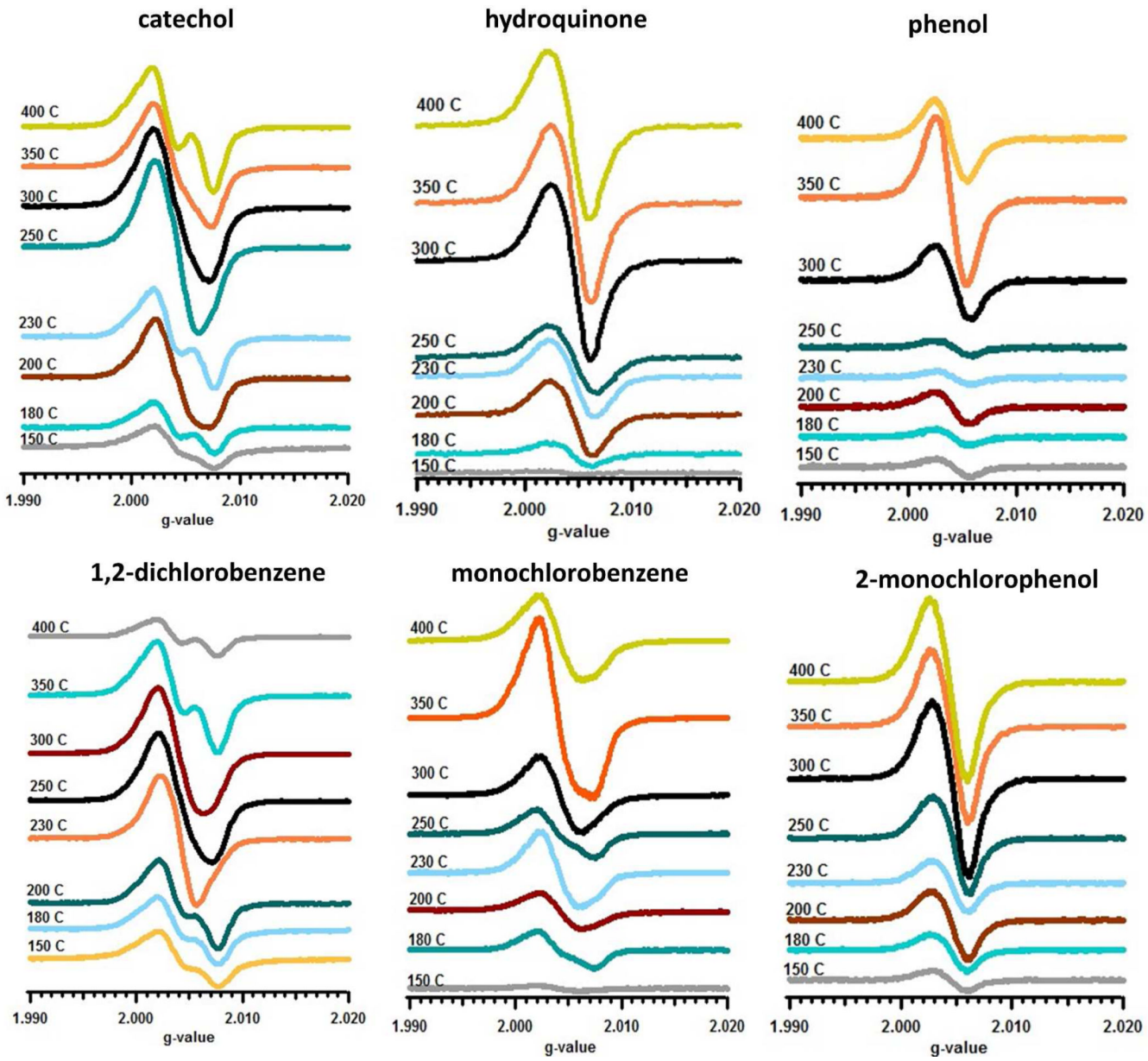

Figure 2.
Temperature dependence of the first-derivative EPR spectra for Ni(II)O for different adsorbates.

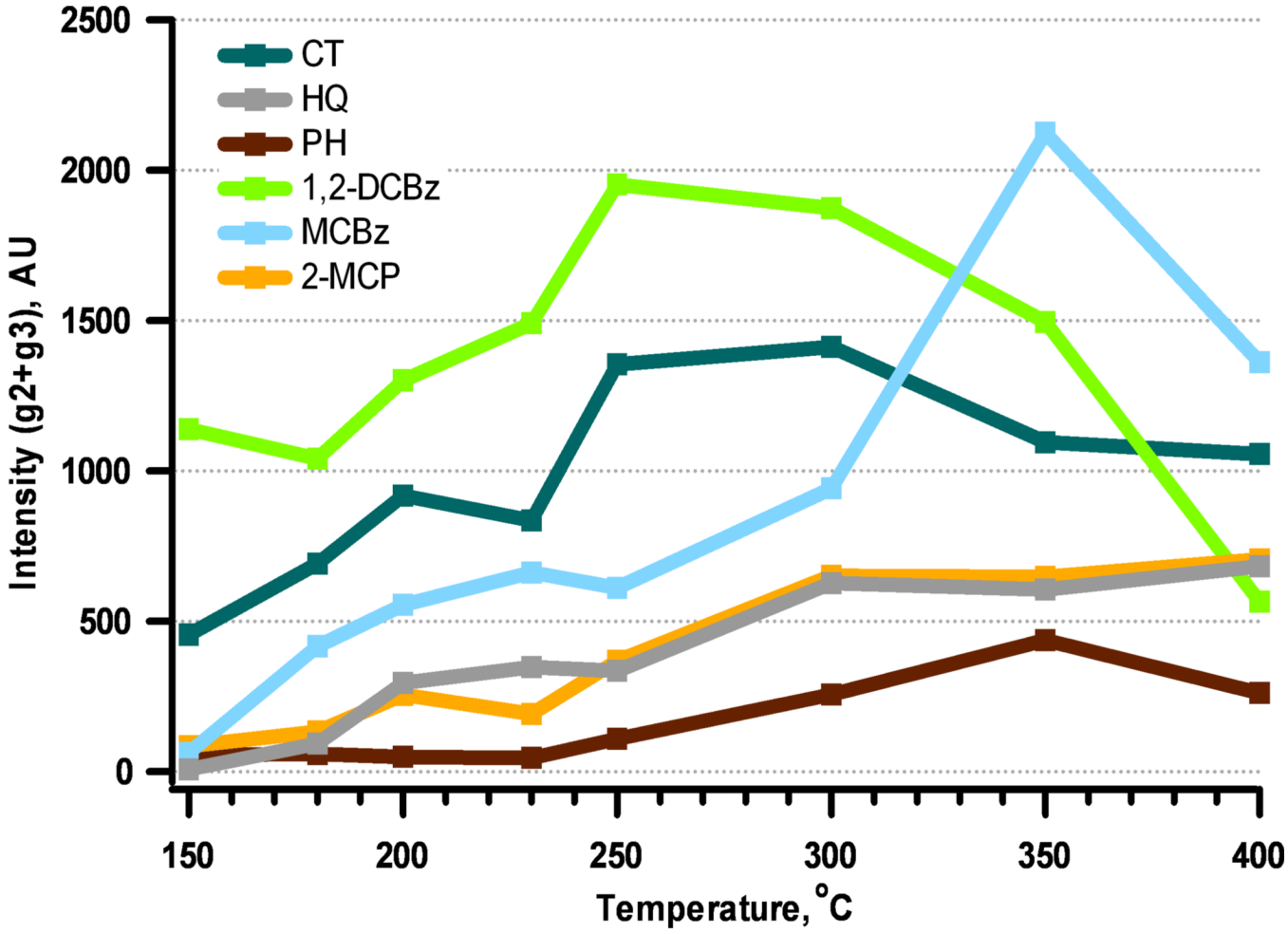

Figure 2.
Total relative concentration of organic EPFRs (g2+g3) adsorbed on 5% Ni(II)O for different adsorbates and dosing temperatures.

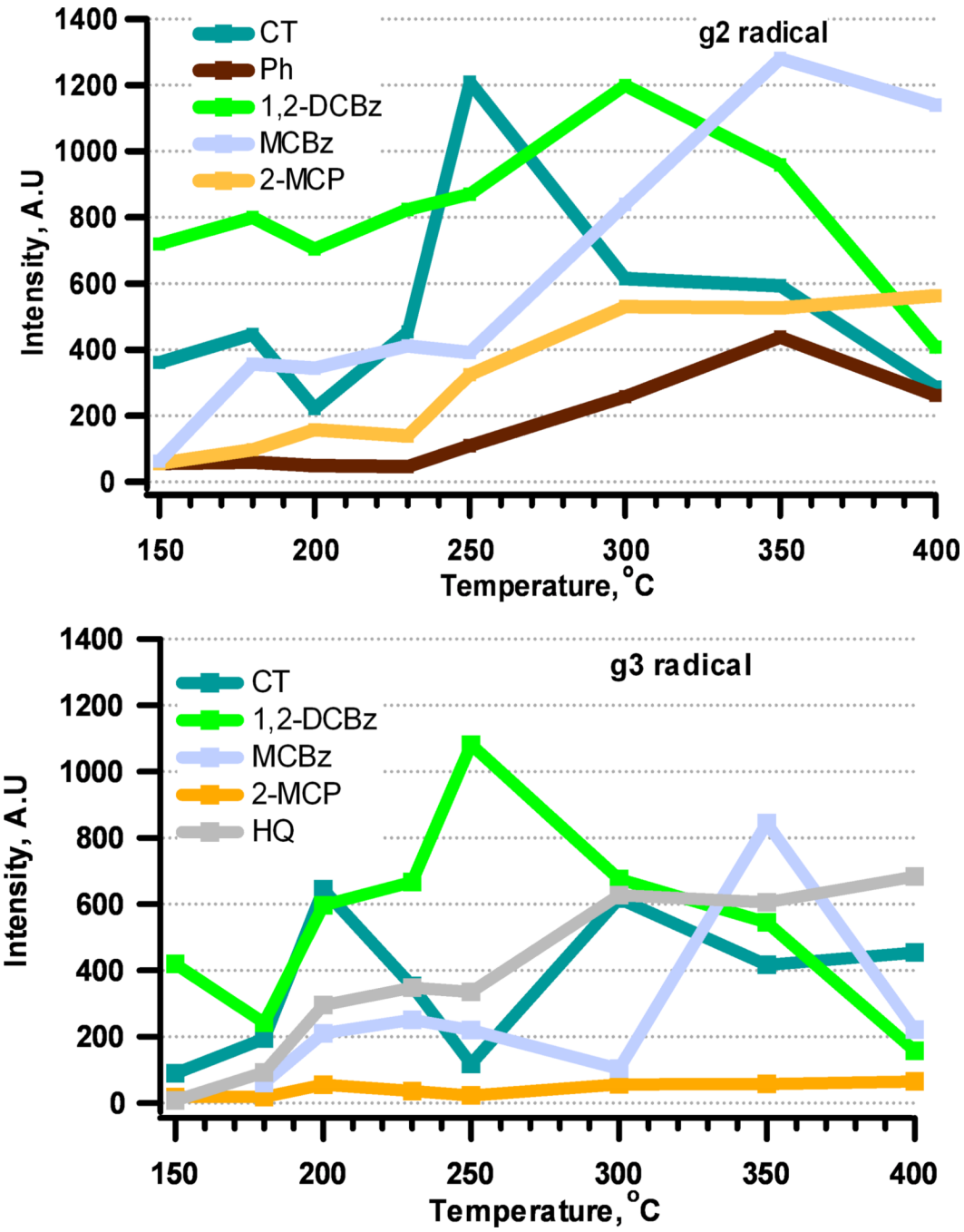

Figure 3.
Yield of the g2 and g3 radicals for different precursors and various dosing temperatures.

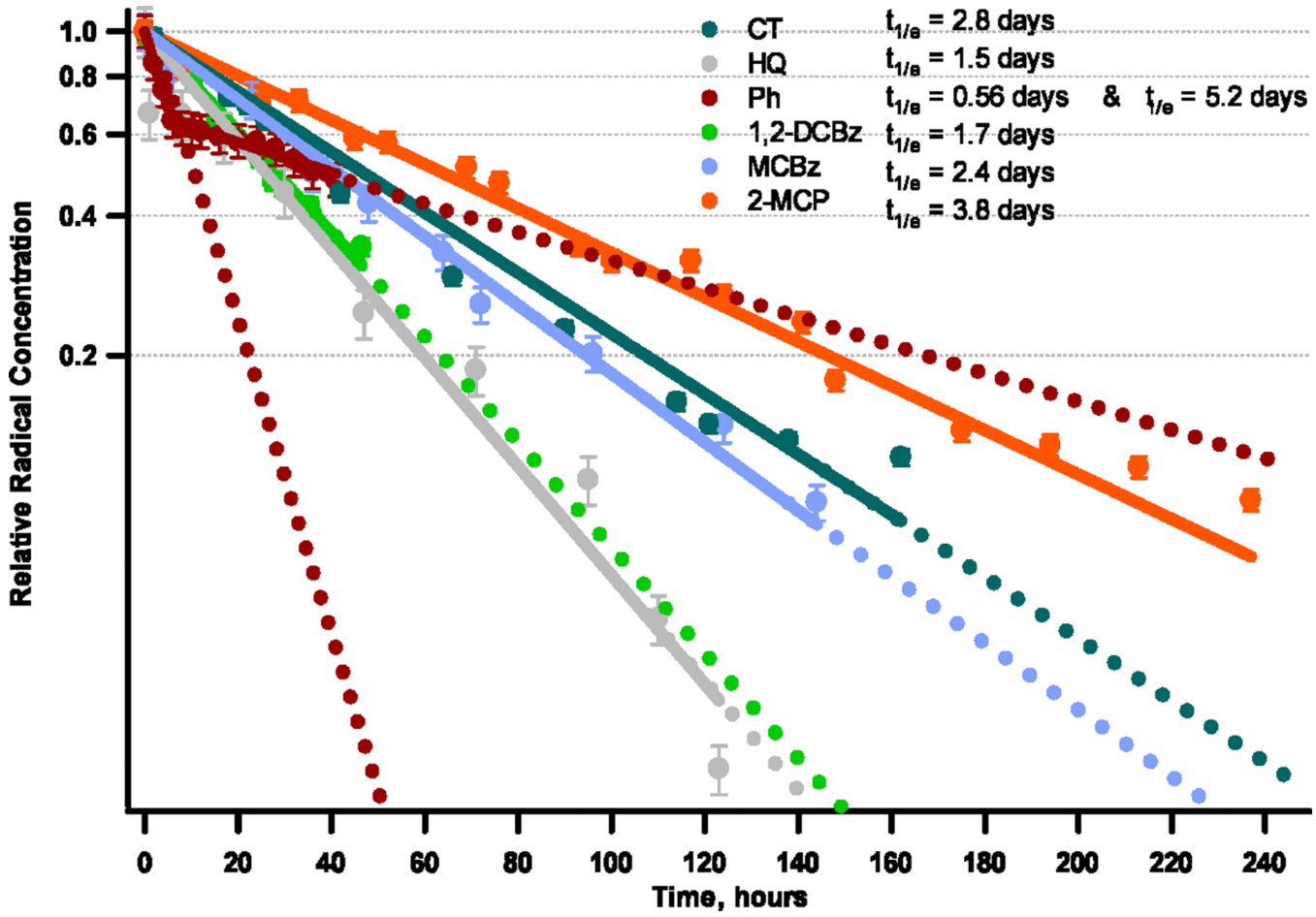

Figure 4.
EPFR disappearance and half-lives in ambient air at room temperature. First-order decay profiles of EPFRs on Ni(II)O /silica surface formed from different adsorbates dosed at 230°C.

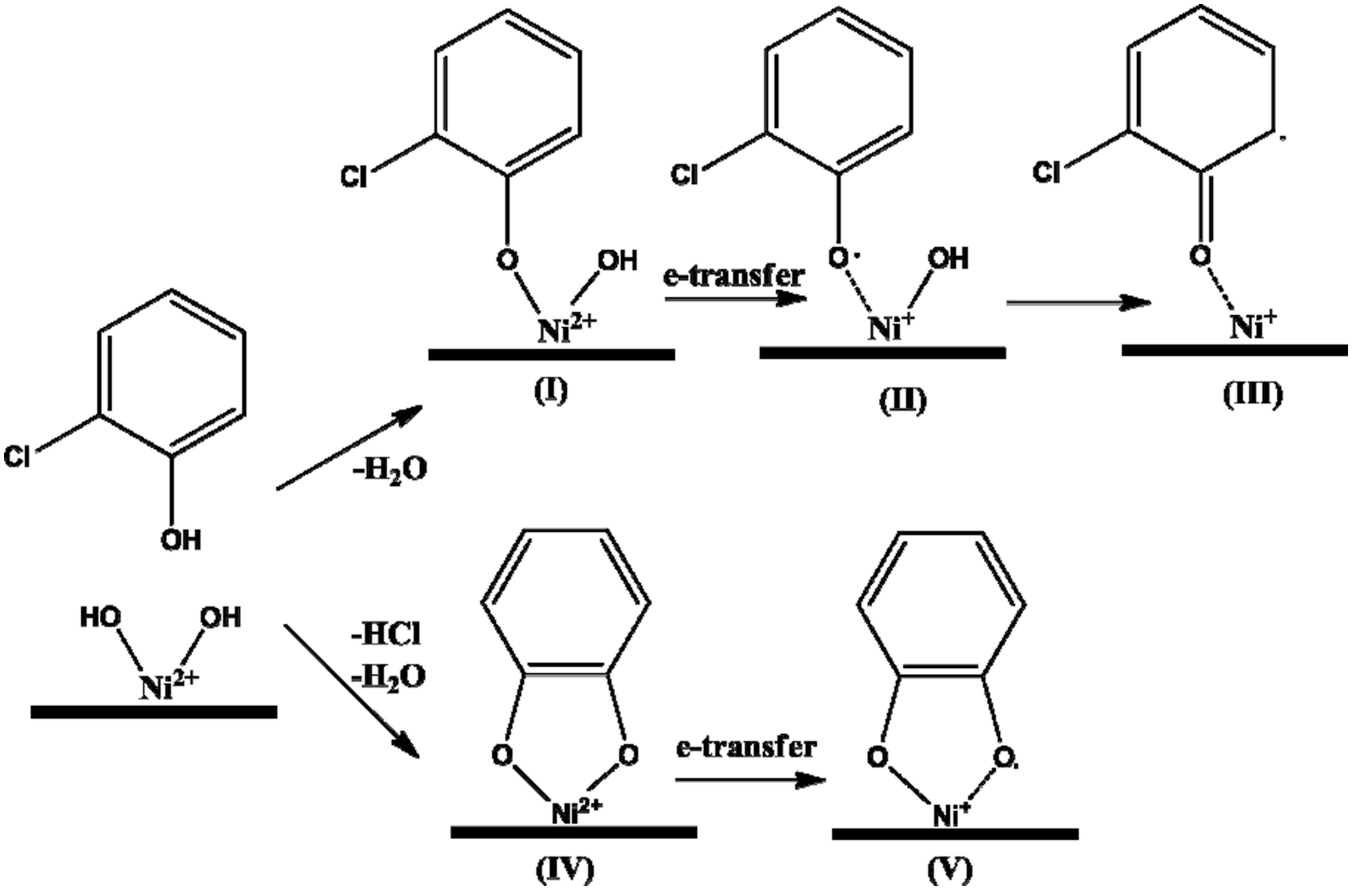

Scheme 1.

General Mechanisms of EPFR Formation from 2-monochlorophenol at Ni^{2+} Sites on a Ni(II)O/Silica Particle.

Table 1

Average g-Values of the Deconvoluted EPR Spectra of Different Adsorbates

	150–300 °C			350–400 °C		
Adsorbate	**g1**	**g2**	**g3**	**g1**	**g2**	**g3**
CT	1.9998	2.0036	2.0064	2.0014	2.0034	2.0061
HQ	2.0000		2.0044	1.9998		2.0050
PH		2.0035	2.0043		2.0040	
1,2-DCBz		2.0035	2.0062		2.0034	2.0064
MCBz	2.0009	2.0031	2.0062	2.0000	2.0038	2.0067
2-MCP	2.0018	2.0044	2.0056	2.0020	2.0045	2.0051

Environ Sci Technol. Author manuscript; available in PMC 2013 September 04.